Journal of Materials Science Research and Reviews

9(4): 36-49, 2022; Article no.JMSRR.90632

Toughness and Ductility Characteristics of Reinforced Concrete Beams Containing Recycled Polyethylene Fibres

Abdullai M. Ghadafi [a*φ] and Charles K. Kankam [b#]

[a] Department of Civil Engineering, Kumasi Technical University, Ghana.
[b] Department of Civil Engineering, KNUST, Kumasi, Ghana.

Authors' contributions

This work was carried out in collaboration between both authors. Both authors read and approved the final manuscript.

Article Information

Open Peer Review History:
This journal follows the Advanced Open Peer Review policy. Identity of the Reviewers, Editor(s) and additional Reviewers, peer review comments, different versions of the manuscript, comments of the editors, etc are available here: https://www.sdiarticle5.com/review-history/90632

Original Research Article

Received 09 June 2022
Accepted 13 August 2022
Published 03 September 2022

ABSTRACT

The paper presents results of investigation on the influence of different volume fractions of polyethylene fibre on the toughness and ductility characteristics of normal strength concrete beams. Nine conventionally reinforced concrete beams measuring 150mm×200mm×2500mm containing 0.25%, 0.50% and 1.0% of polyethylene fibres were cast and tested under a two-point symmetrical loading system using an Avery Denison universal testing machine. Three control beams containing only conventional steel reinforcing bars and measuring 150 mm × 200 mm × 2500 mm were also cast and tested under similar conditions using the same equipment. Throughout the tests, measurements were taken of the loads, mid-span deflections, crack widths and spacings at each load increment until failure. Results of the tests showed that, experimental failure loads for the beams averaged 114% of the theoretical failure loads**,** and failure of the beams was generally governed by the yielding of the tension steel followed by the crushing of concrete in compression. The control specimen possessed higher energy absorption capacity compared to the 0.25% and 0.50% fibre concretes. The 1.0% fibre concrete beams however possessed the highest energy absorption capacity. The ultimate deflections exceeded the predicted deflections on the average by approximately 550% with the ratio of maximum deflection at collapse to deflection at first crack ranging from 9.04 to 59.93. The control specimen exhibited little deflection, averaging

[φ] Lecturer;
[#] Professor;
**Corresponding author: Email: sirghadafi@gmail.com;*

31.7mm and therefore very low ductility prior to collapse compared to the fibre reinforced concrete specimen which averaged 40.1 mm, 41.5 mm, and 46.4mm for 0.25%, 0.50%, and 1.0% fibre reinforced concrete respectively. At failure the fibre reinforced concrete produced more cracks which were closely spaced with visibly smaller crack widths compared to the control beams.

Keywords: Fibre reinforced concrete beams; toughness; ductility; crack width; crack spacing; load; deflection; volume fraction.

1. INTRODUCTION

Concrete is a brittle material with low tensile strength and limited strain capacity [1]. Concrete is also susceptible to cracking and shrinkage, resulting in deterioration and eventual loss of its durability. Fiber reinforced concrete (FRC) is a cement-based composite material reinforced with short, discrete, and usually randomly distributed fibres within a concrete matrix [2]. Fibers are added to bridge discrete microcracks and thereby provide for increased control of the fracture process and also to increase the fracture energy to produce a more ductile behavior [3-5]. In order to ensure durability of concrete, it is very essential to control the crack propagation process and be able to predict the crack pattern (crack width, crack length, and crack spacing). Furthermore, to achieve crack control, large amount of conventional reinforcement is needed, especially in structures where only very small crack widths ($w \leq 0.1$mm) are allowed such as water retaining structures. The bad side to this technique is that: structural dimensions often need to be larger than what is needed for load carrying capacity in order to fit all the steel; heavy labour is required in placing the steel; and also difficulties in pouring the concrete past the tightly packed reinforcement bars in the formwork. By using fibres in combination with or without conventional reinforcement to control cracking however, these drawbacks may be reduced or even eliminated completely.

Several researchers have investigated steel fiber reinforcement in both structural and non-structural concretes to enhance their mechanical and physical properties [6–16]. Other types of fiber materials that are non-ferrous have been used in concrete to achieve similar effects. These include sisal, coconut fibers, coir and oil palm fibers [17–26]. Ghadafi and Kankam [27] found waste polyethylene fiber reinforcement in reinforced concrete beam to be effective enhancer of strength and controller of deformation characteristics.

1.1 Microcracking and the Crack Propagation Process

Concrete is a composite material consisting of two phases: hydrated cement paste and aggregates [28]. Properties of concrete are therefore governed by the properties of the two phases and also by the presence of interfaces between them. Very fine bond cracks exist at the interface between the coarse aggregate and the hydrated-cement paste prior to load application. These cracks result from the differential volume changes between the cement paste and the aggregates due to differences in their stress-strain behavior and also as a result of thermal and moisture movement. These cracks are stable and remain stable at stress levels below 30 percent of the ultimate strength of the concrete. The cracks at this stage do not grow and the stress remains proportional to the strain.

At higher stresses (above 30 percent of ultimate strength of concrete), the stress-strain relation for concrete becomes curvilinear even though the stress-strain relations for the aggregate alone and for the cement paste alone remain linear (Fig. 1). This behavior of concrete can be the result of the development of microcracks. At such higher stress values, the bond cracks at the interface between the two phases begin to increase in length, width, and number. As a consequence, the strain increases at a faster rate than the stress. At this stage, there is a generally slow propagation of microcracks although stable under sustained loading.

At stress levels of 70 to 90 percent of the ultimate strength of concrete, cracks open through the cement paste and the aggregates bridging the bond cracks so that a continuous crack pattern is formed. This stage marks the beginning of faster or rapid propagation of cracks which eventually result in the collapse or failure of the concrete.

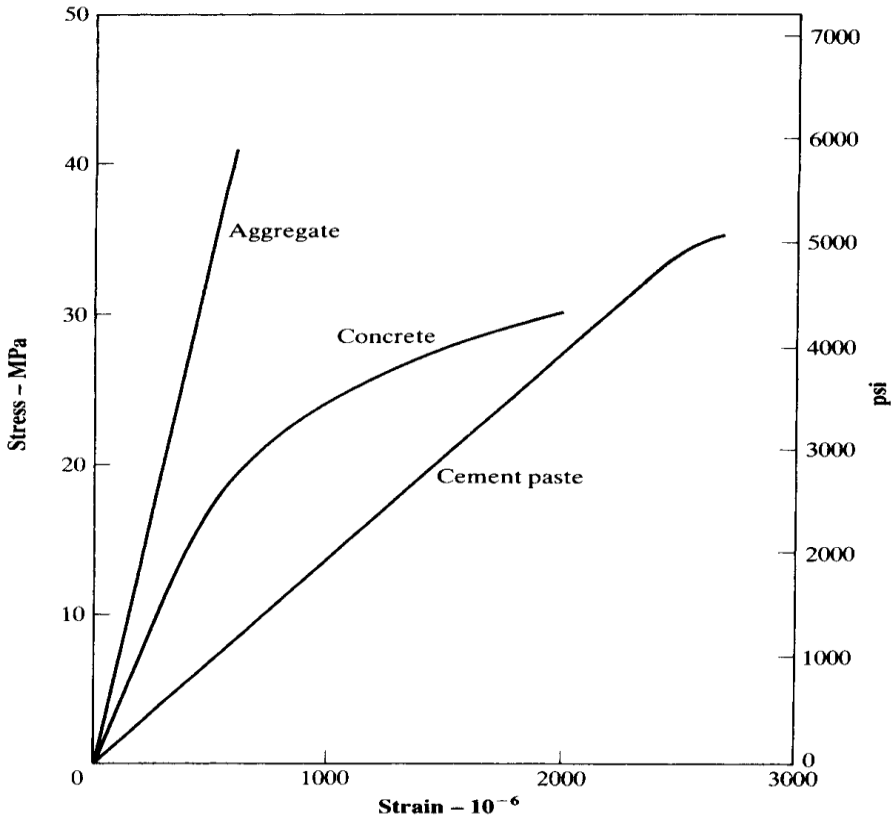

Fig. 1. Stress-strain relations for cement paste, aggregate, and concrete (Neville and Brook, 2010)

1.2 Theory of Strength of Brittle Materials

Concrete is brittle as a result of the brittle nature of the cement paste and the aggregates. The strength of such brittle materials can be determined theoretically using Griffith theory [29] given by

$$\sigma = \sqrt{\frac{2E\gamma}{\pi c}} \quad (1)$$

where σ denotes tensile strength of the concrete; c is size of crack; γ is unit weight of concrete; E is elastic modulus of concrete.

It can be seen from Equation 1 that the tensile strength depends on the size of the crack. Concrete has a lower tensile strength due to the existence of large cracks in the matrix. If the size of the cracks within the matrix can be reduced, the tensile strength of the concrete can be increased. Fibres are therefore used to bridge the cracks thereby preventing the elongation of the cracks and increase of crack width. The purpose of reinforcing the cement-based matrix with fibers is to increase the tensile strength of the matrix by delaying the growth of cracks and also to increase the toughness by transmitting stress across the cracked section so that much larger deformation is possible beyond the peak stress.

2. EXPERIMENTAL METHODS

The post crack flexural toughness was examined under monotonic loading using a two-point symmetrical loading system to provide a central constant moment region and outer shear spans per the American Society of Testing and Materials ASTM C1018 guidelines [30].

2.1 Specimen

A total of twelve reinforced concrete beams measuring 150mm×200mm×2500mm were cast with varying volume fraction of polyethylene fibres as contained in Table 1. Each beam was reinforced in tension using two number 12mm diameter mild steel bars at 25mm from the bottom face. Shear reinforcement in the form of links was provided using 6mm diameter mild steel bars and spaced at 100mm intervals at the

two ends of each beam (ie shear spans) but no stirrups were used in the middle portion (ie constant bending moment region). All beams were designed as under-reinforced section with reinforcement ratio of 0.97 percent.

2.2 Materials

Steel Bars

The mild steel bars used were obtained on the local market and are available in commercial lengths of 9.14m (30feet). The ribbed bars are manufactured from scrap metals by Tema Steel Works (TSW). The yield strength is 370N/mm^2, ultimate strength is 550N/mm^2 and percentage elongation is 10.6. The chemical properties of the steel bars have previously been reported [31].

Cement

The cement used was also procured on the local market. The Diamond brand Ordinary Portland cement (OPC) is of grade 42.5R, fineness 3.4%, consistency 15min, initial and final setting time of 60min and 9 hours, soundness of 2.21 and loss of ignition (LOS) of 1.22.

Coarse Aggregate

The coarse aggregates were obtained from Naachia Quarry Ltd, a local quarry in Kumasi. The angular shaped granite stones of sizes 10mm and 20mm have specific gravity of 2.75kg/m^3, aggregate crushing value of 28.57%, and aggregate impact value of 20.8%.

Fine Aggregate

Fine aggregates were obtained from A. Kanning Ltd in Kumasi. The medium grade silty-sand (river sand) has specific gravity of 2.59kg/m^3, bulk density of 1420kg/m^3, water absorption of 1.7%, percentage sand of 84.21, coefficient of uniformity (Cu) of 14.04 and coefficient of curvature (Cc) of 2.37.

Polyethylene Fibre

Used polyethylene sheets were obtained from local collectors and were cut into pieces measuring 5mm by 40mm and added to the concrete uniformly during mixing. The maximum length of the polyethylene was limited to 40mm so that workability will not be affected. Low density polyethylene (LDPE) with melt flow index of 7g/10min, density of 0.922g/cm^3, low crystallinity (50-60%), elastic modulus of 5GPa, and ultimate strength of 500MPa.

Water

Portable drinking water supplied by Ghana Water Company ltd was used. The water has pH between 6.5-9.0, turbidity less than 5NTU, residual chlorine greater than 0.1mg/l, colour less than 15TCU, total alkalinity of 3.0mg/l, total hardness of 3.0mg/l, E. conductivity of 3µs/cm and E coli count of 0 in 100ml.

Concrete

Medium strength concrete of nominal strength 30N/mm^2 at 28 days was used. The component parts per m^3 were 340kg of ordinary Portland cement, 720kg of river sand, 370kg of 10mm crushed granitic rock, and 720kg of 20mm crushed granitic rock with an optimum water cement ratio of 0.55.

2.3 Casting and Curing of Specimen

Batching of materials was done by weight using an electronic balance of accuracy 0.02kg. A portable electric concrete mixer was used for the mixing to ensure an even, consistent concrete mixture. All of the concrete was batched simultaneously, and the plain and fibre reinforced concretes were then re-mixed for four minutes to ensure the same mixing time was given to each batch. The concrete was compacted by extensive rodding and tamping and cured under damp hessian sacks at 100% relative humidity and 22^{o}C room temperature for 28 days.

2.4 Test Procedure

The beams were simply supported at their ends on the steel beam of the Universal Test Frame (UTF). A two-point symmetrical loading was applied through a spreader beam that formed part of the loading system to produce a constant moment in the central span of the beams. Loading was applied at load increments of 2kN. Deflections at mid-span were measured using dial gauge of accuracy 0.01mm mounted beneath the beam; crack widths were measured on the concrete surface using a crack microscope of accuracy 0.02mm and records of loading was noted from the load gauge attached to the lever pump. At each load increment, all the required measurements were taken.

Table 1. Details of beams

Beam no.	B × D	Vol. fraction of fibre (%)	Span/effective depth ratio	Reinforcement ratio		Concrete strength fcu (N/mm^2)
				Balanced	Actual	
BA1	150 × 200	Nil	13.5	4.69	0.97	37.24
BA2	150 × 200	Nil	13.5	3.96	0.97	29.53
BA3	150 × 200	Nil	13.5	4.26	0.97	32.44
BB1	150 × 200	0.25	13.5	3.41	0.97	25.42
BB2	150 × 200	0.25	13.5	3.16	0.97	23.58
BB3	150 × 200	0.25	13.5	3.82	0.97	28.52
BC1	150 × 200	0.50	13.5	2.83	0.97	21.12
BC2	150 × 200	0.50	13.5	2.91	0.97	21.74
BC3	150 × 200	0.50	13.5	2.73	0.97	20.4
BD1	150 × 200	1.00	13.5	2.59	0.97	19.34
BD2	150 × 200	1.00	13.5	2.23	0.97	16.62
BD3	150 × 200	1.00	13.5	2.31	0.97	17.26

3. THEORETICAL ANALYSIS

The theoretical flexural load P'_{ult} was calculated by considering the three failure scenarios in a reinforced concrete beam, viz;

i. Yielding of the steel in tension;
ii. Crushing of the concrete in compression;
iii. Shear failure.

3.1 Ultimate Flexural Load

For a simply supported beam subjected to two-point symmetrical loading system with a constant moment in the central region, the ultimate flexural load P_{ult} is given by:

$$P'_{ult} = \frac{2(M_{ult} - \frac{\omega}{8}L^2)}{z} \quad (2)$$

where M_{ult} denotes the ultimate moment of resistance; ω is load per unit length due to self-weight of beam; L is span of beam between supports; z is distance from point load to the nearest support.

3.2 Shear Strength

The theoretical shear strength was calculated in accordance with the British Standard BS 8110-1:1997 [32], as follows:

$$V = \left[0.87\frac{A_{sv}f_{yv}}{S_v} + bV_c\right]d \quad (3)$$

where A_{sv} is area of shear links for two legs; S_v is shear link spacing; f_{yv} is tensile strength of shear reinforcement bars; V_c is shear capacity of the concrete. For a one-span simply supported beam, the ultimate shear load, P'_{ult} is given by

$$P'_{ult} = 2V = 2\left[0.87\frac{A_{sv}f_{yv}}{S_v} + bV_c\right]d \quad (4)$$

3.3 Theoretical Deflection

The theoretical deflection of the beams at failure δ'_{ult}, was computed by considering the three distinct stages of loading, viz:

i. Stage 1: Beam deflection under self-weight
ii. Stage 2: Beam deflection under imposed load + self-weight
iii. Stage 3: Combined deflection due to stage 1 and stage 2.

The mid-span deflection of the beams under self-weight was computed from the equation:

$$\Delta_c = \frac{5}{384}\frac{\omega L^4}{E_c I_g} \quad (5)$$

where Δ_c denotes the mid-span deflection of beam; E_c is modulus of elasticity of concrete; I_g is second moment of area of gross section; ω is load per unit length due to self-weight of the beam.

For a simply supported beam that is subjected to a two-point symmetrical loading system, the mid-span deflection can be obtained from the equation

$$\Delta_c = \frac{23}{1296}\frac{PL^3}{E_c I_{cr}} \quad (6)$$

where I_{cr} is second moment of area for a cracked section; P is the ultimate load.

4. TEST RESULTS

Results of the toughness test are presented in Tables 2 and the load-deflection curve in Fig. 3. All twelve beams exhibited similar behavior with the load increasing linearly with the deflection until first crack beyond which there was disproportional increase in deflection compared to the load as cracks propagated. All beams recorded first crack formation within the middle third of the span with majority of the cracks recorded in this region. Failure of beams was generally characterized by yielding of the tension steel followed by the crushing of the concrete in compression.

5. DISCUSSION OF TEST RESULTS

5.1 Post Crack Toughness

Post crack flexural toughness indices were obtained from load-deflection curves. ASTM C1018-89 [8] provides for measurement of ductility by computing the area under the load-deflection curve up to a certain deflection and dividing it by the area under the load-deflection curve up to the first crack deflection. This procedure is well illustrated in Fig. 2.

Areas under the load-deflection curves were obtained by tread-line analysis and curve fitting methods using the EXCEL Solver tool pack.

Relative values of toughness (toughness indices) are then computed as follows:

$$I_5 = \frac{Area\ OACD}{Area\ OAB} \quad (7)$$

$$I_{10} = \frac{Area\ OAEF}{Area\ OAB} \quad (8)$$

$$I_{30} = \frac{Area\ OAGH}{Area\ OAB} \quad (9)$$

Where I_5 represent toughness index corresponding to 3 times of first crack deflection

I_{10} represent toughness index corresponding to 5.5 times of first crack deflection

I_{30} represent toughness index corresponding to 15.5 times of first crack deflection.

The control specimen (beams BA's) outperformed the 0.25% and 0.5% fiber concretes (beams BB's and BC's) by 18 percent and 28 percent respectively as shown in Table 2. However, they underperformed by 23 percent compared to the 1.0 percent fiber concretes (beams BD's). At toughness index I_{10} the control specimen (beams BA's) outperformed the 0.25% fibre concretes (beams BB's) by 23 percent and the 0.5% fibre concretes (beams BC's) by 35 percent, but underperformed by 30% compared to the 1.0 percent fibre concretes (beams BD's). At toughness index I_{30} the control specimen outperformed the 0.25% fibre concretes by 24 percent and the 0.5% fibre concretes by 41 percent but again underperformed by 38% compared to the 1.0 percent fibre concretes.

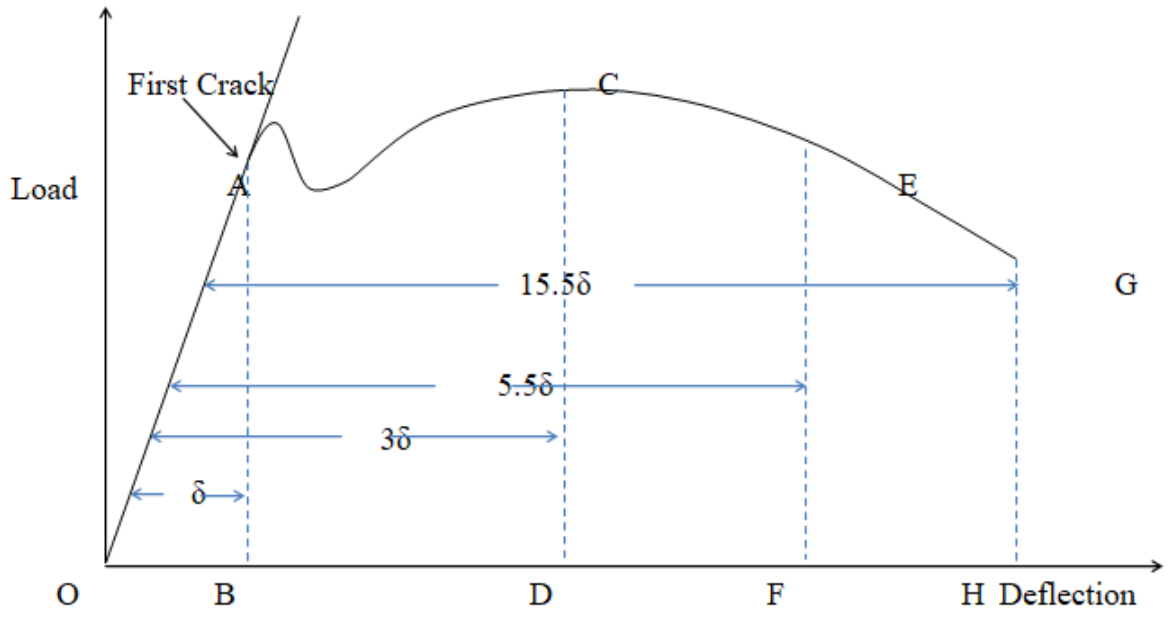

Fig. 2. Analysis of load-deflection curve [8]

Table 2. Post crack flexural toughness indices of control and polyethylene fibre reinforced concrete

type of concrete	First crack load	First crack deflection	Flexural strength	Toughness indices		
	(kN)	(mm)	(Mpa)	I_5	I_{10}	I_{30}
Control	7.67	1.42	6.56	3.9192	8.5663	37.2377
0.25% fibre concrete	7.67	1.4	6.72	3.1743	6.6373	28.0769
0.5% fibre concrete	8.67	1.17	7.48	2.8222	5.6402	21.8119
1.0% fibre concrete	12.67	4.52	8.32	4.7901	11.1556	51.2661

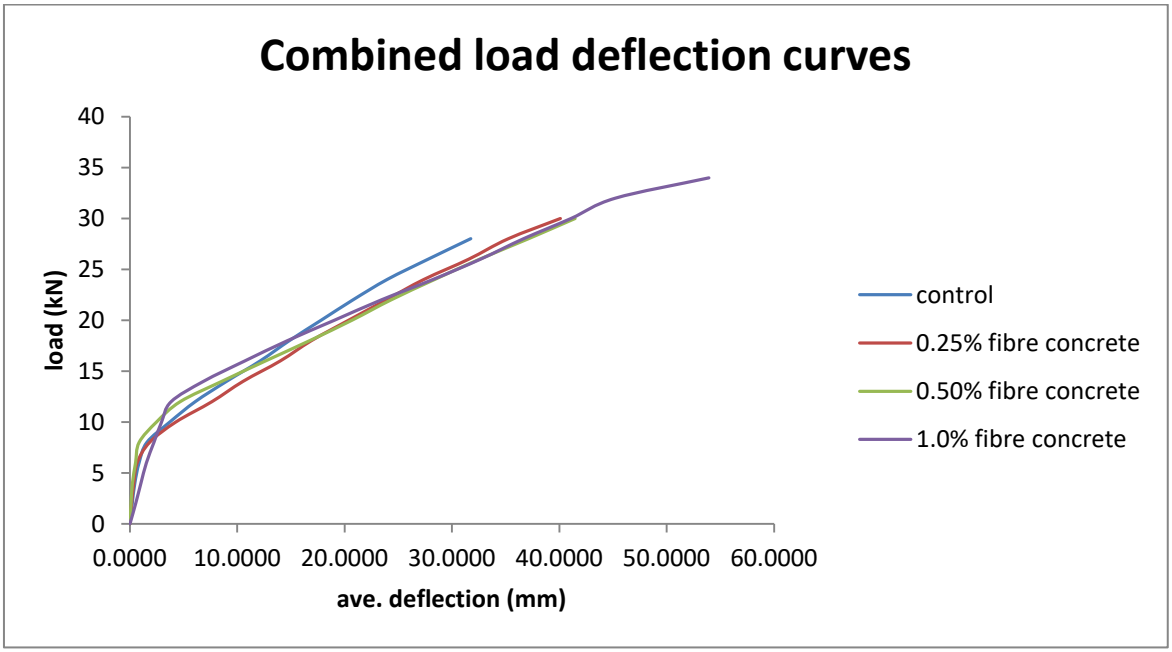

Fig. 3. Load deflection curves for control and fibre reinforced concretes

It is evident therefore that, the control specimen (beams BA's) possess a higher energy absorption capacity at I_5, I_{10}, and I_{30} compared to the 0.25% (beams BB's) and 0.5% (beams BC's) fibre concretes. When a higher fiber volume (1.0%) was used in beams BD's, we had an increase in the energy absorption capacity of the concrete compared to the control specimens.

The possible reason for this is that initially, the entire load was borne by the concrete alone. Immediately after first crack, the fibre and main steel reinforcement which were initially idle began to bear the full load. The ability of the steel and polyethylene fibres to take up the load depends on the concrete-steel and concrete-fibre bond strengths. The concrete-fibre bond strength in turn depends on the quantity of the fibres present in the concrete mix. Pilakoutas et al. (2009) suggested that "bond between concrete and FRP is the most important factor when FRP is used as reinforcement". They went further to say that "sufficient bond must be mobilized between reinforcement and concrete for the successful transfer of load from one to the other".

The low volume fraction of polyethylene fibres and by extension the low bond weakened the concrete and compromised the strength and toughness of the 0.25% and the 0.5% fibre concretes at I_5, I_{10}, and I_{30} compared to the control specimens but the ultimate deflection was unaffected.

5.2 Crack Propagation and Cracking Pattern

Cracks originated from the bottom face of the beam and propagated upwards towards the neutral axis. This resulted in the neutral axis which was originally around the mid-section of the beam moving upward into the compression zone. As loading continued, the neutral axis

continued to move deep into the compression zone towards the upper fibres until the concrete in compression became insufficient to carry any more load. It is quite evident from Figs. 4, 5, 6, and 7 that the cracks went deep into the compression zone and very close to the upper fibres. The researcher therefore concluded that the beams failed in compression due to the inadequacy of the concrete to support any further load after excessive cracking and deflection due to yielding of the reinforcing steel bars in conformity with expected behavior of the beams in line with the under-reinforced design philosophy.

A critical look at Figs. 5, 6, and 7 shows that the fibre concrete had a closer crack distribution than the control beams although they contain the same number of tensile steel reinforcement as the control specimen. The addition of fibres to beams influenced the crack distribution ability of the beams. Measurements of crack widths using crack microscope showed that the crack openings in the fibre reinforced beams were visibly smaller than the crack openings in the control beams as indicated in Table 3. Cracks were closely spaced in the fibre reinforced concrete beams than in the control specimen. Furthermore, it was observed that the fibre reinforced beams provided more cracks than the control beams (Table 3).

It can also be seen from Table 3 that, the 1% fibre reinforced concrete beams withstood a higher load before the appearance of first crack compared to the concrete beams without fibre. This is due to the action of the fibres which were evenly distributed within the matrix interfering with the propagation of micro-cracks. Again, it can be noted from Table 3 that the entire fibre reinforced concrete specimen had a higher ultimate deflection values at higher ultimate loads compared to the control specimen. This is a clear attestation of the superior ductility of the fibre reinforced concrete over the non-fibre reinforced concrete. It has been proven in this study and also in previous studies such as Barris et al (2009), Kim et al (2010), and Fraternalli et al (2011) that fibres interfere with the propagation of micro-cracks by bridging the cracks when the ultimate strain of the concrete is exceeded thereby resulting in concrete with a higher ultimate load carrying capacity.

Fig. 4. Crack propagation of the control specimen

Fig. 5. Crack propagation and characteristics of the 0.25% fibre concrete

Fig. 6. Crack propagation and characteristics of the 0.5% fibre concrete

Fig. 7. Crack propagation and characteristics of the 1.0% fibre concrete

Table 3. Summary of beam loads, deflections and cracking properties

Beam characteristics	Plain concrete	0.25% fibre concrete	0.50% fibre concrete	1.0% fibre concrete
First crack load (kN)	7.67	7.67	8.67	12.67
First crack deflection (mm)	1.42	1.40	1.17	4.52
Ultimate load (kN)	28.00	30.00	30.00	32.67
Ultimate deflection (mm)	31.74	40.11	41.47	46.37
First crack width (mm)	0.08	0.07	0.15	0.36
Biggest crack width at failure (mm)	1.80	1.73	1.43	0.49
Total number of cracks	12.00	12.33	12.67	13.33

5.3 Theoretical and Experimental Loads

The theoretical and experimental loads at first crack and at failure are presented in Table 4. The experimental failure loads P_{ult} were higher and averaged 114% over the predicted failure loads P'_{ult} which were governed solely by the yielding of the tension steel. This is in complete agreement with the actual failure of the beams which was characterized by the yielding of the tensile steel bars followed by the crushing of the concrete in compression after flexural cracks had extended deep into the compression zone. The cracking loads P_{cr} averaged 30% of the experimental failure loads.

The cracking loads P_{cr} averaged 26%, 27%, 29%, and 39% of the experimental failure loads P_{ult} for the 0%, 0.25%, 0.5%, and the 1.0% fibre concrete specimens respectively. This is an indication of the load carrying capacity of the beams after cracking. It is evident that, the 1.0% fibre concrete specimens could carry up to 39% of the first crack load in addition to the first crack load before collapse compared to 26% for the 0% fibre concrete specimens. The analogy here is that if the steel reinforcement alone withstood 26% of the first crack load in addition to the first crack load after the appearance of the first crack in the case of the 0% fibre concrete specimens, then the polyethylene fibres in the fibre reinforced concrete specimens contributed to increase the load carrying capacity to 39% of first crack load in addition to first crack load in the case of the 1.0% fibre concrete specimens.

The shear strength of the beams was approximately two- and- a half times greater than the strength in compression and approximately three- and- a half times their strength in tension.

Table 4. Theoretical and experimental loads

Beam no.	First crack load, P_{cr} (kN)	Experimental failure load, P_{ult} (kN)	Theoretical failure load P'_{ult} (kN)			P_{cr}/P_{ult}	P_{ult}/P'_{ult}
			Steel yielding[a]	Concrete crushing	Shear failure		
BA1	8.00	28.00	28.34	62.03	97.03	0.29	0.99
BA2	7.00	28.00	27.51	48.88	97.03	0.25	1.02
BA3	8.00	28.00	27.88	53.87	97.03	0.29	1.00
BB1	9.00	30.00	27.01	41.99	97.03	0.30	1.11
BB2	8.00	30.00	26.67	38.86	97.03	0.27	1.12
BB3	6.00	30.00	27.46	47.24	97.03	0.20	1.09
BC1	8.00	30.00	26.14	34.69	97.03	0.27	1.15
BC2	9.00	30.00	26.29	35.76	97.03	0.30	1.14
BC3	9.00	30.00	26.00	33.52	97.03	0.30	1.15
BD1	14.00	34.00	25.71	31.71	97.03	0.41	1.32
BD2	12.00	32.00	24.77	27.08	97.03	0.38	1.29
BD3	12.00	32.00	25.02	28.17	97.03	0.38	1.28

[a] *Governing theoretical failure load*

Table 5. Theoretical and experimental deflections

Beam no.	Deflection at first crack δ_{cr} (mm)	Deflection at failure $\delta_{max.}$ (mm)	Theoretical deflection at failure $\delta'_{max.}$ (mm)	$\delta_{max.}/\delta_{cr}$	$\delta_{max.}/\delta'_{max.}$
BA1	1.000	23.750	7.305	23.75	3.25
BA2	1.220	30.380	7.317	24.90	4.15
BA3	2.050	41.100	7.318	20.05	5.62
BB1	2.390	44.000	7.315	18.41	6.02
BB2	0.900	21.800	7.300	24.22	2.99
BB3	0.910	54.540	7.324	59.93	7.45
BC1	1.140	35.100	7.268	30.79	4.83
BC2	1.250	37.520	7.278	30.02	5.15
BC3	1.120	51.800	7.258	46.25	7.14
BD1	5.680	53.920	7.234	9.49	7.45
BD2	3.280	43.600	7.137	13.29	6.11
BD3	4.600	41.600	7.165	9.04	5.81

5.4 Theoretical and Experimental Deflections

The theoretical and experimental deflections of the beams are presented in Table 5. The ultimate deflections exceeded the predicted deflections on the average by approximately 550%. The ratio of maximum deflection at collapse to deflection at first crack ranges from 20.05 to 24.90 for the 0% fibre concrete specimen, 18.41 to 59.93 for the 0.25% fibre concrete specimen, 30.02 to 46.25 for the 0.5% fibre concrete specimen and 19.12 to 32.10 for the 1.0% fibre concrete specimen (Table 5). This is an indication of the ductility of the concrete. The control specimen exhibited little deflection, averaging 31.7mm and very low ductility prior to collapse compared to the fibre reinforced concrete specimen who averaged 40.1mm, 41.5mm, and 46.4mm for 0.25%, 0.50%, and 1.0% fibre reinforced concrete specimen respectively. The larger deflections at greater failure loads recorded for the fibre concrete specimens can be attributed to the action of the fibres interfering with the propagation of micro-cracks in the concrete. The fibres possess much higher ultimate tensile strength (500MPa) and are more ductile compared to the more brittle concrete (4-8MPa) hence their inclusion improves the ductility and tensile strength of the concrete.

The ultimate deflection for the 0% fibre concrete specimen exceeded the predicted deflection on the average by approximately 434%. For the 0.25%, 0.5%, and the 1.0% fibre concrete specimen, the ultimate deflections exceeded the predicted deflections averagely by 549%, 571%, and 646% respectively. The difference between

the theoretical deflection and the experimental deflection in the case of the 0% fibre concrete specimens can be attributed to the properties of the steel bars and the aggregates used for the concrete. The steel bars which are produced from scrap metals have been shown (Kankam and Adom-Asamoah, 2002) to possess a higher tensile strength and very little elongation compared to a standard mild steel bar. In the case of the fibre reinforced concrete specimen, the difference between the theoretical deflection and the experimental deflection can be attributed partly to the properties of the steel bars, the aggregates used and the presence of the fibres in the concrete.

6. CONCLUSION

The toughness, ductility, crack propagation, cracking pattern, theoretical and experimental loads and deflections of control and polyethylene fibre reinforced concrete were investigated. Twelve concrete beams measuring 150×200×2500 mm were tested under a two-point symmetrical loading system using a Universal Test Frame at a constant load increments of 2kN and measurements were taken of the load, mid span deflection, crack width and spacing at each of the load increment. Post crack flexural toughness indices were obtained from load-deflection curves as per the procedure outlined in ASTM C1018. Areas under the load-deflection curve were obtained by trendline analysis and curve fitting methods using the EXCEL solver tool pack.

The experimental failure loads for the beams averaged 114% of the theoretical failure loads and was generally governed by the yielding of the tension steel followed by the crushing of concrete in compression. The 1.0% fibre concrete beams possessed the highest energy absorption capacity averaging 4.79, 11.16, and 51.27 at I_5, I_{10}, and I_{30} respectively. The control specimen exhibited little deflection, averaging 31.7mm and therefore very low ductility prior to collapse compared to the fibre reinforced concrete specimen which averaged 40.1mm, 41.5mm, and 46.4mm for 0.25%, 0.50%, and 1.0% fibre reinforced concrete respectively. At failure the fibre concrete produced more cracks which were closely spaced with visibly smaller crack widths compared to the control beams.

COMPETING INTERESTS

Authors have declared that no competing interests exist.

REFERENCES

1. Hamoush S, Abu-Lebdeh T, and Cummins T. Deflection behavior of concrete beam reinforced with PVA micro-fibers. Construction and Building Materials. 2010; 24:2285-2293.
2. Jansson A. Analysis and design methods for fibre reinforced concrete: A stateof-the-art report. department of civil & environmental engineering, div. of structural engineering/ concrete structures. Chalmers University of Technology. Göteborg, Sweden; 2008.
3. Golpalaratham VS, Getta R. On the characteristics of flexural toughness in fibre reinforced concrete. Cement and Concrete Composites. 1995;17: 239-254.
4. Barris C, Torres LI, Turon A, Baena M, Catalan A. An experimental study of the flexural behavior of GFRP RC beams and comparison with prediction models. Composite Structures. 2009; 9:286-295.
5. Kim SB, Yi NH, Kim HY, Kim JJ, Sung YC. Material and structural performance evaluation of recycled PET fibre reinforced concrete. Cement and Concrete Composites. 2010;32: 232-240.
6. Zaki RA, Abdel Aleem BH, Hassan AAA, Colbourne B. Impact resistance of steel fiber reinforced concrete in cold temperatures. Cement and Concrete Composites. 2021;122:104-116.
7. Luca AM, Sorelli G, Plizzari GA. Steel fiber concrete slabs in ground: A structural material, ACI Structural Journal. 2006; 103.
8. Gao D, Zhu W, Fang D, Tang J, Zhu W. Shear behavior analysis and capacity prediction for the steel fiber reinforced concrete beams with recycled fine aggregate and recycled coarse aggregate. Structures. 2022;37: 44-57.
9. Nassif N, Zeiada W, Al- Khatech G, Haridu S. Attoubat S. Assessment of punching shear strength of fiber-reinforced concrete flat slabs using factorial Design of Experiment. Jordan Journal of Civil Engineering; 16.

10. Kachouh N, El- Maadaroy T, El- Hassan H, El- Ariss B. Shear response of recycled aggregates concrete. Deep Beams containing Steel fibers and web openings. Sustainability. 2022;14.
11. Blanco A, Pujachas P., De la Fuente A, Cavalaro SHP, Aguado A. Assessment of the fibre orientation factor in SFRC slabs. Composites Part B Engineering. 2015; 68:343-354.
12. Ortiz- Lozano JA, Mena-Sebastia F, Segura I, De la Fuente A, Aguado A. Structural use of fiber-reinforced compacting concrete with recycled aggregates. Case study of a foundation wall in Spain. Case Studies in Construction; 2022.
13. Meng S, Jiao C, Ouyang X, Niu Y, FUJ. Effect of steel fiber-volume fraction and distribution on flexural behaviour of ultra-high performance fiber reinforced concrete by digital image correlation technique. Construction and Building Materials. 2022; 320.
14. Toghroli A, Mehrabi P, Shariati M, Trung N.T, Jahandari S, and Rasekh H. Evaluating the use of recycled concrete aggregate and pozzolanic additive in fiber-reinforced previous concrete with industrial and recycled fibers. Construction and Building Materials. 2020;252.
15. Cakir OE, Cetisli F. Behavior of steel fiber reinforced concrete panels in segmental linings. Sustainability. 2022;14.
16. De la Fuente A, Escariz RC, De Figuerido AD, Mulins C, Aguado A. A new design method for steel fibre reinforced concrete pipes. Construction and Building Material. 2012;30:547-555.
17. Venkateshwaran S, Kalalyarrasi ARR. Sisal fiber reinforced concrete. Journal of Emerging Technologies and Innovative Research. 5(6):65-69.
18. Sabarinathan S. A study on mechanical properties of sisal reinforced concrete. Int. Journal of Civil Eng. Special issue; 2017.
19. Ferraz JM, Soares Del Menezzi CH, Teixera DC, Martins SA. Effects of treatment of coir fiber and cement/fiber ratio in properties of cement-bonded composites. Bioresources. 2011; 6(3).
20. Olalusi OB. Mechanical and durability properties of coir fiber reinforced concrete. Journal of Engineering Science and Technology. 14(3):1482-1496.
21. Yalley PP, Kwar A. Use of coconut fibre as an enhancement of concrete. Journal of Engineering Science and Technology. 2012;2:54-69.
22. Kankam CK. The influence of palm stalk fiber reinforcement on the shrinkage stresses in concrete. Journal of Ferrocement. 1994;24(3):249-254.
23. Kankam CK. Impact resistance of palm kernel fiber- reinforced concrete pavement slab. Journal of Ferrocement. 1999;29(4):279-286.
24. Momoh EO, Osofero AI. Recent developments in the application of palm fibers in cement composites. Structural Civil. Eng. 2020;14(1):94-108.
25. Yalley PP, Appiah-Kubi E, Sam A. Strength behaviour of corn husk ash polymer concrete reinforce with coconut fibre. Cogent Engineering. 2021;8(1).
26. Eseg buyota D, Akpokodje O, Uguru H. Physical characteristics and compressive strength of raffia fibre reinforced sandcrete blocks. Information Technology Journal. 2019;6(1):1-8.
27. Ghadafi AM, Kankam CK. Strength characteristics of recycled polyethylene fibre reinforced concrete. Journal of Materials Science Research and Reviews. 2021;7(3):33-41.
28. Neville AM, Brooks JJ. Concrete technology, 2nd Edition. Pearson education limited. Prentice hall. Harlow; 2010.
29. Griffith AA. The phenomena of rupture and flow in solids. Philosophical Transactions of the Royal Society of London. 1921; 221:163-198.
30. American Society for Testing and Materials, ASTM C 1018. Standard Test Method for Flexural Toughness and First Crack Strength of Fibre Reinforced Concrete, American Society for Testing and Materials. West Conshohocken, PA; 1997.
31. Kankam CK, Adom-Asamoah M. Strength and ductility characteristics

of reinforcement steel bars milled from scrap metals. Journal of Materials and Design. 2002;23: 537-545.

32. British Standards, BS 8110-1:1997. Structural use of concrete. Part 1: Code of Practice for design and construction, London; 1997.

Peer-review history:
The peer review history for this paper can be accessed here:
https://www.sdiarticle5.com/review-history/90632